1-Alkyl-2-{(O-Thioalkyl)Phenylazo}Imidazole Complexes of PbII and Their Photochromic Property

ARTICLE *in* ZEITSCHRIFT FÜR ANORGANISCHE CHEMIE · AUGUST 2013

Impact Factor: 1.25 · DOI: 10.1002/zaac.201300173

5 AUTHORS, INCLUDING:

Tapan Kumar Mondal
Jadavpur University
113 PUBLICATIONS **542** CITATIONS
SEE PROFILE

Rajat Saha
Jadavpur University
57 PUBLICATIONS **145** CITATIONS
SEE PROFILE

DOI: 10.1002/zaac.201300173

1-Alkyl-2-{(*O*-Thioalkyl)Phenylazo}Imidazole Complexes of Pb^{II} and Their Photochromic Property

Shefali Saha Halder,[a] Suman Roy,[a] Tapan Kumar Mondal,[a] Rajat Saha,[b] and Chittaranjan Sinha*[a][‡]

Keywords: Pb^{II}-thioalkylphenyl-azoimidazoles; X-ray diffraction; Photochromism; Activation energy; Effect of halide; Halogens

Abstract. Pb^{II} complexes of 1-alkyl-2-{(*o*-thioalkyl)-phenylazo}imidazole (SRaaiNR'), $[Pb(SRaaiNR')_2X_2]$ were characterized by spectroscopic studies. The single-crystal X-ray structure of $[Pb(SEtaaiNEt)_2Cl_2]$ (SEtaaiNEt = 1-ethyl-2-{(*o*-thioalkyl)-phenylazo}imidazole) proved imidazolyl-N and –SEt coordination forming unusual puckered eight member chelate rings. UV light irradiation of the complexes in DMF solution shows E-to-Z (E and Z refer to *trans* and *cis*-configuration about –N=N–, respectively) photoisomerization of the coordinated azoimidazole. The rate of isomerization follows the sequence: $[Pb(SRaaiNR')_2Cl_2] < [Pb(SRaaiNR')_2Br_2] < [Pb(SRaaiNR')_2I_2]$. Quantum yields ($\phi_{E\rightarrow Z}$) and the activation energy (E_a) of the isomerization of the complexes are lower than observed for the free ligand. This can be explained by considering the molecular assembly and the thus observed increase in mass and rotor volume of the complexes. DFT and TDDFT calculations of optimized geometry could explained the spectral properties and photochromic activity.

Introduction

Lead, a useful metal in power, nuclear, construction industries, is a dangerous pollutant[1] to human health. Because of its borderline acidic property it is able to bind strongly with –SH function in enzymes, proteins and also with imidazolyl groups of biomolecules. Interaction of lead with biomolecules may cause toxicity and sometime fatal to human health.[2,3] However, lead may be utilized for the benefit of mankind following the design of proper materials.

Aromatic diazo compounds are useful dyes and pigments and have application in biology, medicine, and in the field of non-linear optics, photoswitching and in the fabrication of optical data storage devices.[4–7] The synthesis and characterization of heteroarylazo dyes have drawn special attention.[8–11] Our interest is to synthesize lead(II) arylazoimidazole compounds. The molecule is π-acidic and its active function is an azoimine group (–N=N-C=N–). We have studied the coordination chemistry[12–16] and analytical application[17,18] of arylazoimidazoles. Our group has recently started to investigate the coordination chemistry of Pb^{II} with 1-alkyl-2-(arylazo)-imidazole.[19,20] One of the interesting properties of arylazoimidazoles and their complexes is photoisomerization,[21–25] which is a reversible transformation between *trans* and *cis* structure of 1-alkyl-2-(arylazo)imidazole about –N=N– upon light irradiation. This is known as photochromic activity. Photochromic compounds have found application in different areas such as liquid crystal alignment,[26] optical data storage,[27] non-linear optics,[28] photoswitching,[29] molecular-photonic devices [30] etc. Use of light as stimulus has enormous advantages over other agents like thermal, magnetic, mechanical, electrical, redox etc. Light irradiation to some molecules may reversibly transform one molecular structure to other structure whose absorption spectra differ prominently.[31]

In continuation of our efforts, this work is concerned with the photoisomerization of Pb^{II} complexes of 1-alkyl-2-{(*o*-thio-alkyl)phenyl-azo}imidazole (SRaaiNR') (Scheme 1). The ligand is unusually chelated via imidazolyl-N and -SR to Pb^{II}. Ligand, SRaaiNR', has three potential donor centers, N(imidazole), N(azo) and –SR, and can serve as tridentate-N,N',S [32] and bidentate-N,N' [25] donor agent. Single-crystal X-ray structure determination of representative complex confirmed the structure of the complex. Light irradiation of solutions of

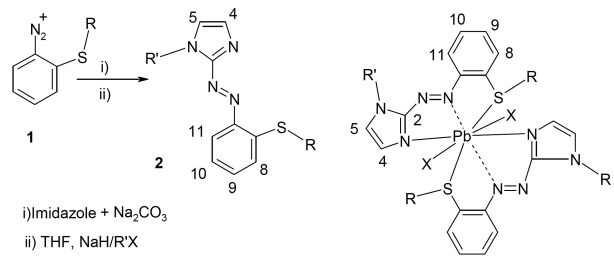

$[Pb(SRaaiNR')_2X_2]$ (X = Cl (**3**), Br (**4**), I (**5**))

R = R' = Me (**a**); R = Me, R' = Et (**b**); R = Et, R' = Me (**c**); R = R' = Et (**d**))

Scheme 1. Synthesis of ligand and atom numbering of the ligand and the complexes.

* Prof. Dr. C. Sinha
E-Mail: c_r_sinha@yahoo.com
[a] Department of Chemistry
Jadavpur University
Kolkata – 700 032, India
[b] Department of Physics
Jadavpur University
Kolkata – 700 032, India
[‡] Present Address: Kalyani Govt. Engg. College
Kalyani, Nadia
West Bengal – 741235, India

the complexes showed reversible photoisomerization.[25,32] The effect of Pb–X (X = Cl, Br, I) and SRaaiNR' on photoisomerization rate and quantum yields have been reported in this work. Theoretical calculation has been attempted on optimized geometry of the complexes to rationalize the bonding and spectral properties of the complexes.

Results and Discussion

Syntheses of the Complexes

1-Alkyl-2-{(*o*-thioalkyl)phenylazo}imidazoles [SRaaiNR'] (R = R' = Me (**2a**); R = Me, R' = Et (**2b**); R = Et, R' = Me (**2c**); R = R' = Et (**2d**)] were synthesized by literature procedure.[32] The reaction of hot water solution or EGME solution of PbX_2 and the ligand SRaaiNR' in MeOH in 1:2 molar ratio yielded orange-red crystals of composition $[Pb(SRaaiNR')_2X_2]$. Microanalytical data confirmed the composition of the complexes. The structures were established by single-crystal X-ray diffraction studies.

Structure of [Pb(SEtaaiNEt)$_2$Cl$_2$] (3d)

The molecular structure of **3d** is shown in Figure 1. The structure shows interesting unusual $N_{imidazole}$ (N), S–Et eight-membered metal coordination whereas N_{azo} (N') is weakly bonded and appears as an in-between N,S-chelator, 1-ethyl-2-{(*o*-thioethyl)phenylazo}, SEtaaiNEt. The charge balance is carried out by two Pb–Cl bonds. Thus, the Pb^{II} atom shows $PbN_2S_2Cl_2$ coordination whereas the two N_{azo} atoms are weakly bonded (Pb–N_{azo}, 3.151/3.090 Å) as evident from sum of their van der Waals radii (Pb 2.02; N_{azo} 1.55 Å; sum of van der Waals radii = 3.57 Å) and the low chelate angle (vide infra). The Pb–N(1)–C(7)–N(3)–N(4)–C(1)–C(2)-S(1) puckered chelate ring is essentially nonplanar (deviation > 0.14 Å). The bond parameters are listed in Table 1. The Pb–$N_{imidazole}$ (N(1/5)) bonds are sufficiently strong and the distances are comparable with lengths reported in literature.[20] The Pb–S bond lengths are Pb(1)–S(1/2), 3.351/3.338 Å.[33,34] The N_{azo} atoms (N(4/8)) could be forced to bind to Pb^{II} and the Pb(1)–N(4/8) (3.151/3.090 Å) bond lengths are much longer than previously reported distances (2.752(12) Å,[20]) which is also unfavorable due to the small chelate angles (∠N(1)–Pb(1)–N(4), 55.81°; ∠N(5)–Pb(1)–N(8), 53.81°). Thus, an eight-membered chelated structure may be considered. The Pb–S(–R) bonding

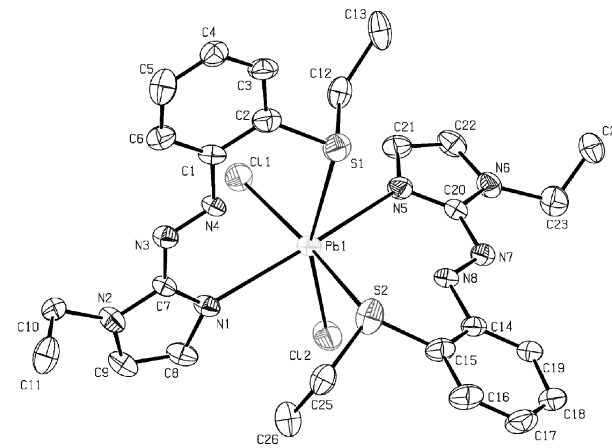

Figure 1. ORTEP plot (40% probability ellipsoid) of $[Pb(SEtaaiNEt)_2Cl_2]$ (**3d**).

Table 1. Selected bond lengths /Å and angles /° for $[Pb(SEtaaiNEt)_2Cl_2]$ (**3d**).

Bond length /Å	$[Pb(SEtaaiNEt)_2Cl_2]$ # Expt.	Theo.	$[Pb(SEtaaiNEt)_2Cl_2]$ † Theo.	$[Pb(SEtaaiNEt)_2Br_2]$† Theo.	$[Pb(SEtaaiNEt)_2I_2]$† Theo.
Pb(1)–N(1)	2.631(7)	2.656	2.666	2.682	2.688
Pb(1)–N(5)	2.654(7)	2.707	2.713	2.698	2.713
Pb(1)–X(1)	2.669(3)	2.609	2.611	2.824	3.075
Pb(1)–X(2)	2.638(3)	2.611	2.609	2.822	3.081
Pb(1)–S(1)	3.351(3)	3.814	3.918	3.801	3.720
Pb(1)–S(2)	3.338(2)	3.938	3.766	3.877	3.775
N(3)–N(4)	1.245(9)	1.267	1.267	1.267	1.268
N(7)–N(8)	1.272(9)	1.268	1.268	1.268	1.268
S(1)–C(2)	1.793(12)	1.780	1.837	1.781	1.780
S(1)–C(12)	1.441(8)	1.839	1.781	1.839	1.838
Bond angle /°					
	Expt.	Theo	Theo	Theo	Theo
N(1)–Pb(1)–X(2)	83.99(17)	83.65	83.52	85.68	87.22
N(1)–Pb(1)–N(5)	164.0(2)	161.6	160.56	165.0	169.94
X(2)–Pb(1)–N(5)	86.11(19)	85.22	84.68	84.86	85.85
N(1)-Pb(1)- X(1)	85.42(17)	85.19	84.59	85.38	87.22
X(2)–Pb(1)–X(1)	96.26(12)	102.91	102.6	104.37	105.53
N(5)–Pb(1)–X(1)	83.16(17)	83.06	82.98	85.73	88.78
C(20)–N(5)–Pb(1)	122.0(6)	123.07	123.08	125.55	125.7
C(21)–N(5)–Pb(1)	128.9(7)	127.3	127.08	125.99	126.66
C(7)–N(1)–Pb(1)	124.1(5)	124.63	124.88	125.82	125.57
C(8)–N(1)–Pb(1)	129.4(7)	127.33	127.11	125.95	126.38

†SEtaaiNEt acts as monodentate $N_{imidazole}$ donor. # SEtaaiNEt acts as bidentate $N_{imidazole}$,$S_{thioether}$ chelator

Zeitschrift für anorganische und allgemeine Chemie ZAAC Journal of Inorganic and General Chemistry

is confirmed by ^1H NMR spectroscopy; the signals of –S–Me/Et are shifted downfield compared with free ligand data.[32]

The $[Pb(N,S)_2Cl_2]$ units are connected by hydrogen bonding with Pb–Cl bonds of imidazolyl-H/aryl-H of neighboring molecules to constitute supramolecular networks (Figure 2 and Figure 3). Out of two Pb–Cl bonds the Cl(1) atom is triply hydrogen bonded, Cl(1)···H(5), H(9), H(22) and Cl(2) is doubly hydrogen bonded Cl(2)···H(4), H(19). The bonding parameters are Cl(1)···H(5)–C(5):C(5)–H(5), 0.93(4) Å, Cl(1)···H(5), 2.73(2) Å, C(5)···Cl(1), 3.633(15) Å; ∠Cl(1)···H(5)–C(5), 164.31(1)° (symmetry, *–x*, *–y*, 1*–z*); Cl(1)···H(9)–C(9):C(9)–H(9), 0.93(2) Å, Cl(1)···H(9), 2.80(6) Å, C(9)···Cl(9), 3.632(11) Å and ∠Cl(1)···H(9)–C(9), 149.5(1)° (symmetry, *–x*, *–*1*–y*, 1*–z*); Cl(1)···H(22)–C(22):C(22)–H(22), 0.93(1) Å, Cl(1)···H(22), 2.73(7) Å, C(22)···Cl(1), 3.570(12) Å and ∠Cl(1)···H(22)–C(22), 149.5(6)° (symmetry, *–x*, *–*1*–y*, 2*–z*); and Cl(2)···H(4)–C(4):C(4)–H(4), 0.93(3) Å, Cl(2)···H(4), 2.74(3) Å, C(4)···Cl(2), 3.557(15) Å and ∠Cl(2)···H(4)–C(4), 146.62(1)° (symmetry, *x*, 1+*y*, *z*); Cl(2)···H(19)–C(19):C(19)–H(19), 0.93(1) Å, Cl(1)···H(19), 2.77(8) Å, C(19)···Cl(2), 3.554(12) Å and ∠Cl(2)···H(19)–C(19), 141.48(1)° (symmetry, *–*1*–x*, *–*1*–y*, 2*–z*). These interactions form 2D supramolecular sheet within the ***ab***-plane, Figure 2**.** (symmetry: *–x*, *–y*, 1*–z*, *x*, 1+*y*, *z*). These 2D sheets are further connected by π···π interaction with thioaryl and imidazole rings (C(13)–H(13C)···Cg4; H···Cg4, 2.80 and ∠C(13)–H(13C)···Cg4, 137°. C(23)–H(23B)···Cg4; H···Cg4, 2.82 and ∠C(23)–H(23B)···Cg4, 144° (Cg4 refers to thioaryl group, C(14) to C(19)) to form 3D supramolecular structure, Figure 3.

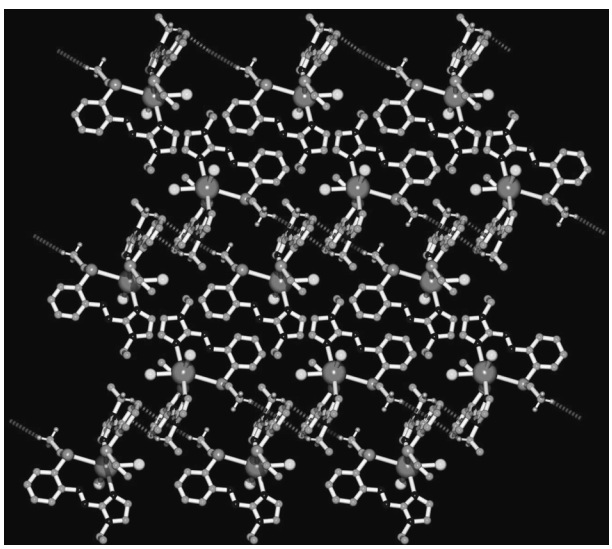

Figure 2. 2D supramolecular sheet of **3d** formed by C–H···π interactions.

DFT computations were carried out with optimized geometries of the complexes. The bond parameters are calculated and comparison of calculated and X-ray crystallographically determined bond lengths and angles show good agreement (Table 1). The theoretical bond lengths are elongated by 0.02–0.6 Å than that of X-ray determined structures. The molecular functions are calculated and the electronic structure is assigned to the molecule that was used to consign electronic transitions observed in solution spectra. SEtaaiNEt has three donor centers – N_{azo}, $N_{imidazole}$, $S_{thioether}$ and could act as monodentate $N_{imidazole}$ ($Pb(N_{imidazole})_2Cl_2$) or bidentate $N_{imidazole}$, $S_{thioether}$ chelator ($Pb(N_{imidazole}, S_{thioether})_2Cl_2$) or tridentate N_{azo}, $N_{imidazole}$, $S_{thioether}$ chelators ($Pb(N_{imidazole}, N_{azo}, S_{thioether})_2Cl_2$) (Figure 4). DFT calculations were performed for three isomeric structures of $[Pb(SEtaaiNEt)_2Cl_2]$ (3d). The calculation shows that the energy of the bidentate $N_{imidazole}$, $S_{thioether}$ chelated complex (energy of X-ray structure, –86215.9917 eV) is closer to a proposed monodentate $N_{imidazole}$ coordinated structure (–86215.9928 eV) while the energy of the tridentate N_{azo}, $N_{imidazole}$, $S_{thioether}$ coordinated compound has higher energy (–86187.554 eV). This results partly suggest remote feasibility of tridentate behavior of SEtaaiNEt to Pb^{II}. However, both monodentate $N_{imidazole}$ coordinated ($Pb(N_{imidazole})_2Cl_2$) and bidentate $N_{imidazole}$, $S_{thioether}$, chelated ($Pb(N_{imidazole}, S_{thioether})_2Cl_2$) complexes could exist and only the latter could be structurally characterized. The procedure has been extended to $[Pb(SEtaaiNEt)_2Br_2]$ and $[Pb(SEtaaiNEt)_2I_2]$ (*Supporting Information, Figure S2 and Figure S3*) and the molecular functions are calculated to explain the spectral and photochromic properties.

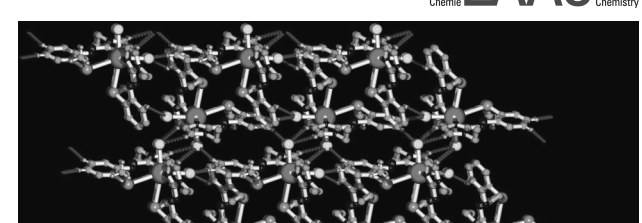

Figure 3. 3D supramolecular structure formed by hydrogen bonding interactions. Each monomeric units are connected by supramolecular C–H···π interactions leading to the formation of 2D supramolecular sheet structure, Hydrogen bonding interactions also connect the monomeric units to form 3D supramolecular structure.

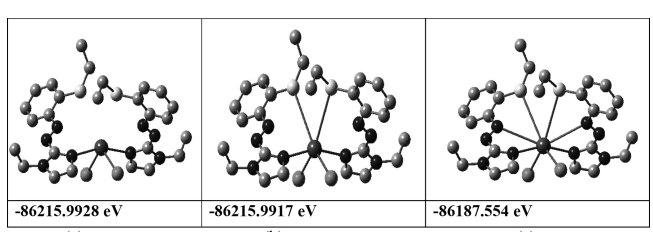

Figure 4. Optimized structures of (a) monodentate $N_{imidazole}$ coordinated, (b) bidentate $N_{imidazoles}$, $S_{thioether}$ chelated and (c) $N_{imidazoles}$, N_{azo}, $S_{thioether}$ tridentate type $[Pb(SEtaaiNEt)_2Cl_2]$.

UV/Vis Spectra and Photochromism

The solution electronic spectra of the compounds were recorded in DMF in 200–600 nm. There are two bands in the UV/Vis region at 360–370 and 410–420 nm. By comparison with the spectra of the free ligands[32] and those of the Pb^{II} complexes,[19,20] it may be concluded that these stem from intramolecular charge-transfer transitions (n→π*, π→π*). These observations are also supported by frontier molecular orbital calculations using X-ray diffraction parameters.

The electronic configurations of three representative complexes [Pb(SEtaaiNEt)$_2$X$_2$] (X = Cl (**3d**), Br (**4d**), I (**5d**)) were calculated by DFT and TD-DFT computation. The molecular functions have been used to explain the origin of transitions**.** The selected MOs of the complexes are shown in Figure 5 and composition of MOs is given in the *Supporting Information, Tables S1, S3, S5*. The HOMOs of these three complexes are composed of lead (15 % **3d** and **4d** while 9 % for **5d**), SEtaaiNEt (49 %, **3d**; 33 %, **4d**; 7 %, **5d**) and halogen (36 % of Cl in **3d**; 52 % of Br in **4d** and 84 % of I in **5d**) (*Supporting Information, Table S1*). Other occupied MOs (HOMO-1, HOMO-2 etc) are composed of SEtaaiNEt and X (halogen). The LUMOs (LUMO, LUMO+1, LUMO+2 etc.) are π* orbital delocalized over the entire SEtaaiNET (98–100 %). The energy of the MOs is correlated in Figure 6. The calculated transitions are given in Table 2 (Details are given in the *Supporting Information*, *Tables S2, S4, S6*). The intensity of these transitions has been assessed from oscillator strength (*f*). The calculated bands are mainly contributed of ILCT, XLCT or admixture of them and a small contribution of MLCT (MLCT, metal-to-ligand charge transfer; XLCT, halide-to-ligand charge transfer, ILCT, intraligand charge transfer where ligand refers to SEtaaiNEt). The transitions in UV region (< 400 nm) are the mixture of ILCT and XLCT. The observed transitions appear closer to the calculated wavelength in the complexes (Figure 7).

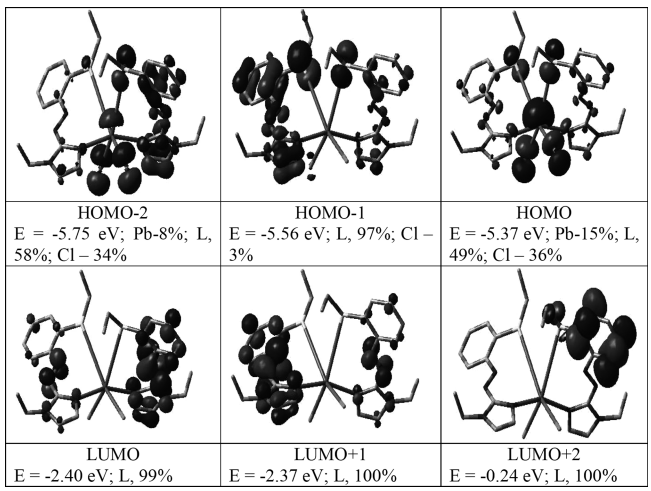

Figure 5. Selected MOs (HOMO-2, HOMO-1, HOMO, LUMO, LUMO+1, LUMO+2) of [Pb(SEtaaiNEt)$_2$Cl$_2$] (**3d**).

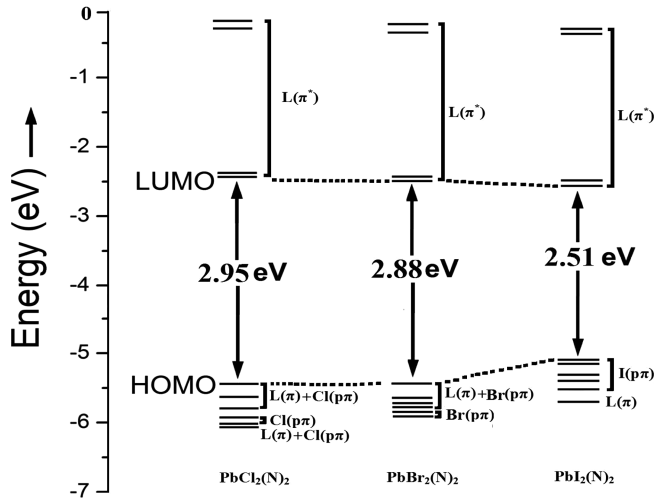

Figure 6. Correlation amongst calculated energy levels of [Pb(SEtaaiNEt)$_2$X$_2$] (X = Cl (**3d**), Br (**4d**), I (**5d**)).

Table 2. Selected list of excitation energies of the complexes in gas phase and the assignment of transitions.

Excitation energy /eV	Wavelength /nm	f	Key Transitions	Character
[Pb(SEtaaiNEt)$_2$Cl$_2$] (**3d**)				
2.3626	524.77	0.0238	(83 %)HOMO→LUMO	ILCT, XLCT
2.3931	518.09	0.0255	(79 %) HOMO→LUMO+1	ILCT, XLCT
2.7401	452.47	0.0567	(69 %) HOMO-1→LUMO	ILCT
2.8594	433.61	0.0552	(74 %) HOMO-2→LUMO	ILCT, XLCT
4.6498	266.64	0.0541	(88 %) HOMO→LUMO+2	ILCT, XLCT
4.7774	259.52	0.1002	(78 %) HOMO→LUMO+3	ILCT, XLCT
4.8737	254.40	0.0771	(50 %) HOMO-1→LUMO+2	ILCT
[Pb(SEtaaiNEt)$_2$Br$_2$] (**4d**)				
2.2831	543.06	0.0137	(92 %)HOMO→LUMO	ILCT, XLCT
2.3199	534.44	0.0162	(91 %) HOMO→LUMO+1	ILCT, XLCT
4.5371	273.27	0.0226	(83 %) HOMO→LUMO+2	ILCT, XLCT
4.7862	259.05	0.0516	(68 %) HOMO-1→LUMO+2	ILCT, XLCT
4.8673	254.73	0.0309	(81 %) HOMO-2→LUMO+2	ILCT, XLCT
4.9416	250.90	0.1082	(72 %) HOMO→LUMO+4	ILCT, XLCT
[Pb(SEtaaiNEt)$_2$I$_2$] (**5d**)				
4.0986	302.50	0.0309	(40 %) HOMO→LUMO+2	XLCT
4.2712	290.28	0.0016	(35 %) HOMO-3→LUMO+2	XLCT
4.6360	267.44	0.0462	(26 %) HOMO-4→LUMO+2	XLCT
4.7248	262.41	0.0172	(30 %) HOMO-4→LUMO+3	XLCT

Zeitschrift für anorganische und allgemeine Chemie ZAAC Journal of Inorganic and General Chemistry

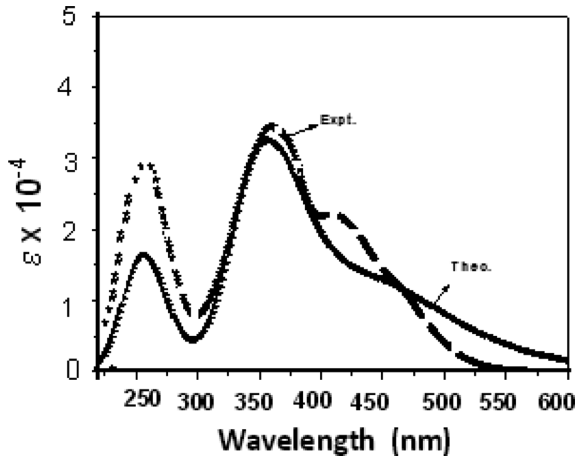

Figure 7. UV/Vis Spectrum (theoretical,___; experimental (DMF solution),---) of $[Pb(SEtaaiNEt)_2Cl_2]$.

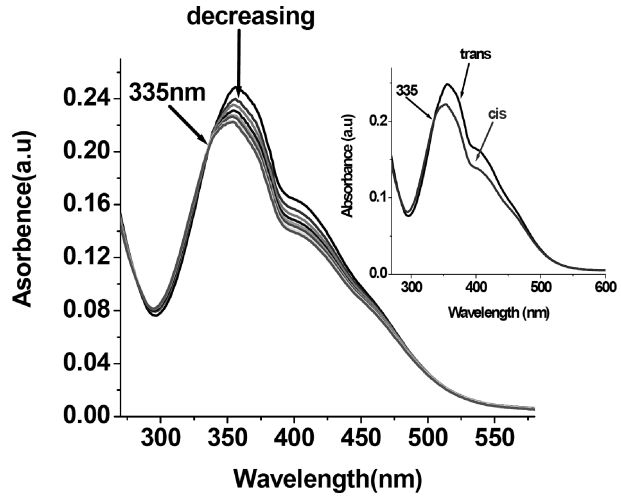

Figure 8. Spectral change of $[Pb(SEtaaiNEt)_2Cl_2]$ (**3d**) in DMF upon repeated irradiation at 360nm at 4 min interval at room temperature.

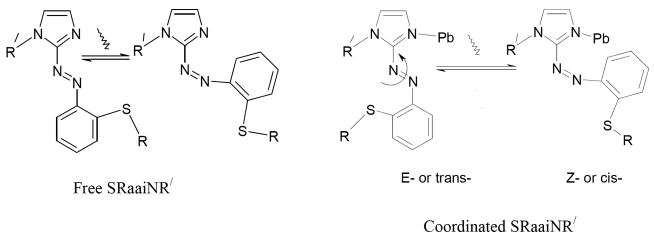

Scheme 2. Photochromism of free and coordinated $SRaaiNR^{/}$.

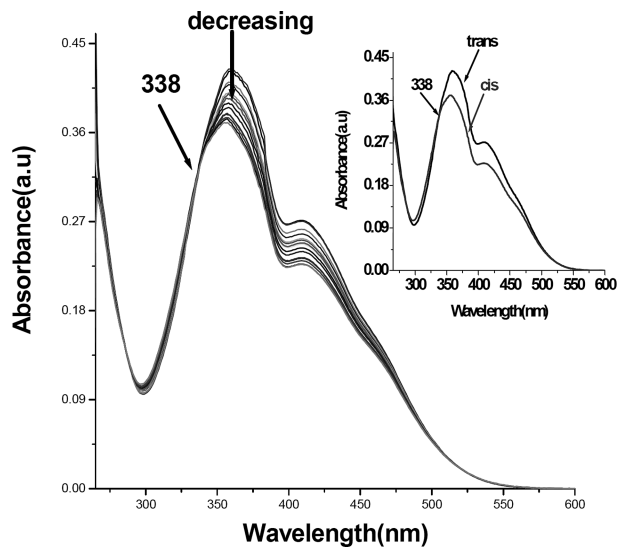

Figure 9. Z → E isomerization of $[Pb(SMeaaiNEt)_2Cl_2]$ (**3b**).

The E-to-Z (*trans*-to-*cis*) isomerization of free ligand, SRaaiNR' in acetonitrile (Figure 8) and $[Pb(SRaaiNR')_2X_2]$ (Scheme 2) was investigated by irradiation of UV light in DMF solution (Figure 9). The spectral pattern of free ligands (SRaaiNR') and their Pb^{II} complexes are very similar. Being no transition metal ion, Pb^{II} does not contribute to the electronic configuration of coordinated SRaaiNR', except the energies of the FMOs (frontier molecular orbitals) are reduced and hence electronic spectral transitions are shifted to longer wavelengths by 5–10 nm. Photoisomerization of SRaaiNR' was carried out in acetonitrile. Because of very close polarity of DMF (6.4 D) and acetonitrile (5.8 D) the photoisomerization of SRaaiNR' has been taken in acetonitrile and has compared with results of DMF solution of the complexes. Absorption spectra of the E-configuration of coordinated SRaaiNR' in the complexes, **3–5**, in DMF are changing with isosbestic point upon excitation to the *cis* configuration of the ligand. The quantum yields were measured for the E-to-Z ($\phi_{E\rightarrow Z}$) photoisomerization of these compounds in DMF on irradiation of UV wavelength (Table 3). The $\phi_{E\rightarrow Z}$ values are significantly dependent on the nature of the substituents, halide type and molecular weight.[19,20,22–25] In presence of -Me and -Et groups, the quantum yields are reduced compared to those of the free ligands.

Upon UV light irradiation, the *trans* (E) structure of SRaaiNR' changed to *cis* structure about the azo (–N=N–) function and the *cis* molar ratio reached to >80% (Scheme 2). UV light irradiation to the solution of the photochrome may insist the rotation of the azo-aryl group (–N=N–Ar) which isomerizes from *trans* (E) to *cis* (Z) form. The rates of photoisomerization (*trans*-to-*cis* (E-Z), $\phi_{E\rightarrow Z}$) increases with decreasing electronegativity of X in the complexes (Table 3); rate follows $[Pb(SRaaiNR')_2Cl_2]$ (**3**) < $[Pb(SRaaiNR')_2Br_2]$ (**4**) < $[Pb(SRaaiNR')_2I_2]$ (**5**) although the molar mass follows the order **3**<**4**<**5**. Higher electronegativity of chlorine in **3** may help to enhance association strength by electrostatic interaction with neighboring molecules and may effectively increase rotor mass than that of **4** or **5**.

The thermal Z–to–E (*cis*-to-*trans*) isomerization of the complexes was followed by UV/Vis spectroscopy in MeCN at varied temperatures, 298–313 K and the activation energies were obtained (Table 4) from Eyring plots (Figure 10). In the complexes the E_as are quite closer to respective free ligands, which mean slow rate of Z-to-E thermal isomerization of the complexes. The entropies of activation (ΔS^*) are more negative in the complexes than that of the free ligands. This is also de-

Table 3. Excitation wavelength ($\lambda_{\pi\pi^*}$), rate of E(*trans*)→ Z(*cis*) conversion and quantum yield ($f_{t\rightarrow c}$).

Compd	λ_{π,π^*} /nm	Isobastic points/nm	Rate of E→ Z conversion × 10^8 /s^{-1}	($f_{E\rightarrow Z}$).
SMeaaiNMe♣	357	337	4.908 (2)	0.317 (1)
SMeaaiNEt♣	358	337	3.108 (4)	0.232 (3)
SEtaaiNMe♣	357	336	4.67 (1)	0.290 (4)
SEtaaiNEt♣	356	335	2.948 (2)	0.197 (4)
$[Pb(SMeaaiNMe)_2Cl_2]$ (**3a**)	362	341	2.83 (2)	0.151 (3)
$[Pb(SMeaaiNEt)_2Cl_2]$ (**3b**)	361	342	1.67 (3)	0.091 (6)
$[Pb(SEtaaiNMe)_2Cl_2]$ (**3c**)	362	340	2.12 (2)	0.093 (7)
$[Pb(SEtaaiNEt)_2Cl_2]$ (**3d**)	360	338	1.13 (9)	0.086 (8)
$[Pb(SMeaaiNMe)_2Br_2]$ (**4a**)	361	343	3.34 (5)	0.176 (2)
$[Pb(SMeaaiNEt)_2Br_2]$ (**4b**)	364	339	1.82 (7)	0.098 (7)
$[Pb(SEtaaiNMe)_2Br_2]$ (**4c**)	363	341	2.45 (4)	0.103 (1)
$[Pb(SEtaaiNEt)_2Br_2]$ (**4d**)	363	340	1.48 (5)	0.092 (8)
$[Pb(SMeaaiNMe)_2I_2]$ (**5a**)	360	342	3.62 (3)	0.203 (6)
$[Pb(SMeaaiNEt)_2I_2]$ (**5b**)	361	341	2.07 (4)	0.105 (1)
$[Pb(SEtaaiNMe)_2I_2]$ (**5c**)	360	339	2.81 (1)	0.111 (5)
$[Pb(SEtaaiNEt)_2I_2]$ (**5d**)	362	340	1.72 (4)	0.099 (5)

Data are collected from Ref. [24].

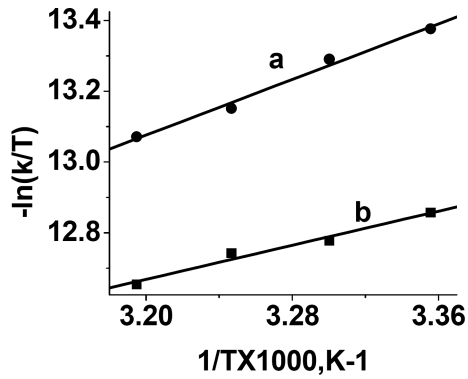

Figure 10. Eyring plots of *cis*-to-*trans* thermal isomerization of (a) SEtaaiNEt (**2d**) and (b) $[Pb(SEtaaiNEt)_2Cl_2]$ (**3d**).

fending the increase in rotor volume in the complexes. It is our apprehension that light irradiation in UV wavelength (360–364 nm) may cleave Pb–SR bonds while Pb^{II}–$N_{imidazole}$ may remain in hooking stage (as it is a stronger bond than Pb–SR) and pendant thioalkylarylazo unit may suffer bond rotation to assist photochromism. DFT and TD-DFT computation have calculated that the transitions in UV region (< 400 nm) are the mixture of ILCT and XLCT which assist for photochromic reaction. Participation of X in the π···π* transition has indirectly influencing the E-to-Z photoisomerization.

Experimental Section

Materials

$PbCl_2$, $PbBr_2$ and PbI_2 were obtained from Loba Chemicals, Bombay, India 1-alkyl-2-{(*o*-thio-alkyl)phenylazo}imidazole were synthesized by reported procedure.[32] All other chemicals and solvents were reagent grade as received.

Physical Measurements

Microanalytical data (C, H, N) were collected on Perkin–Elmer 2400 CHNS/O elemental analyzer. Spectroscopic data were obtained using the following instruments: UV/Vis spectra with a Perkin–Elmer Lambda 25 spectrophotometer. IR spectra (KBr disk, 4000–200 cm^{-1}) with a Perkin–Elmer RX-1 FTIR spectrophotometer; photoexcitation experiments were carried out using a Perkin–Elmer LS-55 spectrofluorimeter.

Syntheses

$[Pb(SEtaaiNEt)_2Cl_2]$ (3d): A methanol solution of 1-ethyl-2-{(*o*-thioethyl)phenylazo}imidazole (56 mg, 0.20 mmol) was added in drops to hot water solution of $PbCl_2$ (30 mg, 0.11 mmol) and stirred for 2 h and heated to reflux for 2 h. The resultant reddish solution was collected by filtration. Slow evaporation of the solution gave orange-red crystals in a yield of 53.42 mg (62%).

$[Pb(SRaaiNR')_2X_2]$ (X = Br and I) were synthesized by mixing solutions of $PbBr_2$ and PbI_2 in EGME (ethylene glycol monomethyl ether) and SRaaiNR' in MeOH. The products were isolated in yields in the range 60–70%.

$[Pb(SRaaiNR')Br_2]$ and $[Pb(SRaaiNR')I_2]$ were synthesized following a similar procedure using $PbBr_2$ and PbI_2 and SRaaiNR' in methanol-EGME solution (3:1, v/v) under reflux.

Microanalytical data of the complexes were as follow $[Pb(SMeaaiNMe)_2Cl_2]$ (**3a**) Anal. Found: C, 35.59; H, 3.22; N, 15.08%. Calc. for $[PbC_{22}H_{24}N_8S_2Cl_2]$: C, 35.58; H, 3.23; N, 15.09 %. **FT-IR** (KBr disc), ν(N=N), 1420; ν(C=N), 1571 cm^{-1}. **UV/Vis** (DMF) (λ_{max}(nm)(10^{-3} ε (dm^3 mol^{-1} cm^{-1}): 362 (26.21), 410 (17.65). **^{1}H NMR** (300 MHz, $CDCl_3$), δ(ppm), (J(Hz)): 7.41 (br. s, 4-H), 7.24 (br. s, 5-H), 7.35 (d, 7.0 Hz, 8-H), 7.44 (m, 9- and 10-H), 8.10 (d, 8.0 Hz, 11-H), 4.32 (s, 1-CH_3), 2.60 (s, S-CH_3).

$[Pb(SMeaaiNEt)_2Cl_2]$ (3b): Anal. Found: C, 37.38; H, 3.64; N, 14.55%. Calc. for $[PbC_{24}H_{28}N_8S_2Cl_2]$: C, 37.40; H, 3.63; N, 14.54 %. **FT-IR** (KBr disc), ν(N=N), 1425; ν(C=N), 1572 cm^{-1}. **UV/Vis** (DMF) (λ_{max}(nm)(10^{-3} ε (dm^3 mol^{-1} cm^{-1}): 361 (28.45), 411(19.09). **^{1}H NMR** (300 MHz, $CDCl_3$), δ(ppm), (J(Hz)): 7.42 (br. s, 4-H), 7.23 (br. s, 5-H), 7.32 (d, 7.0 Hz, 8-H), 7.43 (m, 9- and 10-H), 7.98 (d, 8.0 Hz,11-H), 4.48 (q, 6.60 Hz, 1-CH_2), 1.65 (t, 7.30 Hz, (1-CH_2)-CH_3)), 2.67 (s, S-CH_3).

$[Pb(SEtaaiNMe)_2Cl_2]$ (3c): Anal. Found: C, 37.41; H, 3.62; N, 14.52%. Calc. for $[PbC_{24}H_{28}N_8S_2Cl_2]$: C, 37.40; H, 3.63; N, 14.54 %.

Table 4. Rate and activation parameters for Z → E thermal isomerization.

Compd	*T* /K	Rate of thermal Z → E conversion × 10^4 /s^{-1}	E_a /kJmol^{-1}	Δ*H** /kJ·mol^{-1}	Δ*S** /J·mol^{-1}K^{-1}	Δ*G** /kJ·mol^{-1}
3a	298	7.14	16.03	13.49	–259.93	77.47
	303	7.854				78.77
	308	8.671				80.07
	313	9.752				81.37
3b	298	7.385	14.68	12.14	–264.12	78.72
	303	8.198				80.04
	308	8.75				81.36
	313	9.91				82.68
3c	298	7.401	14.93	12.39	–263.27	78.46
	303	8.212				79.78
	308	8.785				81.1
	313	9.978				82.41
3d	298	7.768	12.55	10.01	–270.84	80.72
	303	8.555				82.07
	308	9.008				83.43
	313	10.00				84.78
4a	298	7.266	18.15	15.61	–252.66	75.31
	303	8.081				76.57
	308	9.147				77.83
	313	10.30				79.1
4b	298	7.533	16.64	14.1	–257.43	76.73
	303	8.312				78.02
	308	9.241				79.30
	313	10.4				80.59
4c	298	7.587	16.89	14.35	–256.52	76.46
	303	8.347				77.74
	308	9.367				79.02
	313	10.5				80.30
4d	298	7.899	14.77	12.23	–263.23	78.45
	303	8.819				79.77
	308	9.461				81.09
	313	10.6				82.40
5a	298	7.312	20.11	17.57	–246.04	73.34
	303	8.145				74.57
	308	9.512				75.8
	313	10.7				77.03
5b	298	7.611	18.16	15.62	–252.22	75.18
	303	8.491				76.44
	308	9.589				77.70
	313	10.8				78.96
5c	298	7.647	18.35	15.81	–251.57	74.98
	303	8.511				76.24
	308	9.601				77.50
	313	10.9				78.76
5d	298	7.995	15.24	12.70	–261.57	77.96
	303	8.892				79.27
	308	9.641				80.58
	313	10.8				81.88

FT-IR (KBr disc), ν(N=N), 1427; ν(C=N), 1573 cm^{-1}. **UV/Vis** (DMF) (λ_{max}(nm)(10^{-3} ε (dm^3 mol^{-1} cm^{-1}): 362 (27.21), 412 (20.52). **^{1}H NMR** (300 MHz, $CDCl_3$), δ(ppm), (J(Hz)): 7.40 (br. s, 4-H), 7.23 (br. s, 5-H), 7.34 (d, 7.0 Hz, 8-H), 7.46 (m, 9- and 10-H), 7.94 (d, 7.9 Hz, 11-H), 4.28 (s, 1-CH_3), 3.01 (q, 7.2 Hz, S-CH_2), 1.31 (t, 7.35 Hz, (S-CH_2)-CH_3).

[Pb(SEtaaiNEt)$_2$Cl$_2$]: (3d): Anal. Found: C, 39.07; H, 4.02; N, 14.04 %.Calc. for [$PbC_{26}H_{32}N_8S_2Cl_2$]: C, 39.09; H, 4.01; N, 14.03 %. **FT-IR** (KBr disc), ν(N=N), 1490; ν(C=N), 1572 cm^{-1}. **UV/Vis** (DMF) (λ_{max}(nm)(10^{-3} ε (dm^3 mol^{-1} cm^{-1}): 360 (34.60), 409 (22.26). **^{1}H NMR** (300 MHz, $CDCl_3$), δ(ppm), (J(Hz)): 7.41 (br. s, 4-H), 7.22 (br. s, 5-H), 7.35 (d, 7.0 Hz, 8-H), 7.45 (m, 9- and 10-H), 7.97 (d, 8.0 Hz, 11-H), 4.59 (q, 6.7 Hz, 1-CH_2), 1.60 (t, 7.2 Hz, (1-CH_2)-CH_3), 3.04 (q, 7.2 Hz, S-CH_2), 1.39 (t, 7.36 Hz, (S-CH_2)-CH_3).

[Pb(SMeaaiNMe)$_2$Br$_2$] (4a): Anal. Found: C, 31.76; H, 2.90; N, 13.49 %. Calc. for $PbC_{22}H_{24}N_8S_2Br_2$: C, 31.77; H, 2.89; N, 13.48 %. **FT-IR** (KBr disc), ν(N=N), 1421; ν(C=N), 1622 cm^{-1}. **UV/Vis** (DMF) (λ_{max}(nm)(10^{-3} ε (dm^3 mol^{-1} cm^{-1}): 361 (18.55), 410 (18.11). **^{1}H NMR** (300 MHz, $CDCl_3$), δ(ppm), (J(Hz)): 7.40 (br. s, 4-H), 7.23 (br. s, 5-H), 7.36 (d, 7.0 Hz, 11-H), 7.55 (m, 9- and 10-H), 7.84 (d, 8.0 Hz), 4. 72 (s, 1-CH_3), 2.55 (s, S-CH_3).

[Pb(SMeaaiNEt)$_2$Br$_2$] (4b): Anal. Found: C, 33.54; H, 3.25; N, 13.02 %. Calc. for $PbC_{24}H_{28}N_8S_2Br_2$: C, 33.53; H, 3.26; N, 13.04 %. **FT-IR** (KBr disc), ν(N=N), 1422; ν(C=N), 1621 cm^{-1}. **UV/Vis** (DMF) (λ_{max}(nm)(10^{-3} ε (dm^3 mol^{-1} cm^{-1}): 364 (31.59), 410 (21.32). **^{1}H NMR** (300 MHz, $CDCl_3$), δ(ppm), (J(Hz)): 7.41 (br. s, 4-H), 7.20 (br. s, 5-H), 7.33 (d, 7.0 Hz, 8-H), 7.52 (m, 9- and 10-H), 7.88 (d,

8.0 Hz,11-H), 4.47 (q, 7.0 Hz, 1-CH_2), 1.69 (t, 7.30 Hz, (1-CH_2)-CH_3)), 2.64 (s, S-CH_3).

[Pb(SEtaaiNMe)$_2$Cl$_2$] (4c): Anal. found: C, 33.52; H, 3.27; N, 13.03 %. Calc. for $PbC_{24}H_{28}N_8S_2Cl_2$: C, 33.53; H, 3.26; N, 13.04 %. **FT-IR** (KBr disc), ν(N=N), 1419; ν(C=N), 1573 cm^{-1}. **UV/Vis** (DMF) (λ_{max}(nm)(10^{-3} ε (dm^3 mol^{-1} cm^{-1}): 363 (26.05), 411 (21.58). **^{1}H NMR** (300 MHz, $CDCl_3$), δ(ppm), (J(Hz)): 7.42 (br. s, 4-H), 7.20 (br. s, 5-H), 7.35 (d, 7.0 Hz, 8-H), 7.56 (m, 9- and 10-H), 7.83 (d, 8.0 Hz, 11-H), 4.30 (s, 1-CH_3), 3.00 (q, 7.4 Hz, S-CH_2), 1.30 (6.2 Hz, (S-CH_2)-CH_3).

[Pb(SEtaaiNEt)$_2$Br$_2$] (4d): Anal. found: C, 35.18; H, 3.60; N, 12.61 %. Calc. for $PbC_{26}H_{32}N_8S_2Br_2$: C, 35.17; H, 3.61; N, 12.62 %. **FT-IR** (KBr disc), ν(N=N), 1420; ν(C=N), 1590 cm^{-1}. **UV/Vis** (CH_3CN) (λ_{max}(nm)(10^{-3} ε (dm^3 mol^{-1} cm^{-1}): 363 (31.42), 408 (22.68). **^{1}H NMR** (300 MHz, $CDCl_3$), δ(ppm), (J(Hz)): 7.41 (br. s, 4-H), 7.22 (br. s, 5-H), 7.32 (d, 7.0 Hz), 7.53 (m, 9- and 10-H), 7.86 (d, 8.0 Hz, 11-H), 4.52 (q, 7.25 Hz, 1-CH_2), 1.62 (t, 7.2 Hz, (1-CH_2)-CH_3), 3.04 (q, 7.3 Hz, S-CH_2), 1.35 (t, 6.16 Hz, (S-CH_2)-CH_3).

[Pb(SMeaaiNMe)$_2$I$_2$] (5a): Anal. found: C, 28.55; H, 2.60; N, 12.10 %. Calc. for $PbC_{22}H_{24}N_8S_2I_2$: C, 28.54; H, 2.59; N, 12.11 %. **FT-IR** (KBr disc), ν(N=N), 1412; ν(C=N), 1535 cm^{-1}. **UV/Vis** (DMF) (λ_{max}(nm)(10^{-3} ε (dm^3 mol^{-1} cm^{-1}): 360 (16.11), 411 (15.45). **^{1}H NMR** (300 MHz, $CDCl_3$), δ(ppm), (J(Hz)): 7.41 (br. s, 4-H), 7.28 (br. s, 5-H), 7.31 (d, 7.0 Hz, 8-H), 7.55 (m, 9- and 10-H), 7.80 (d, 8.0 Hz, 11-H), 4.14 (s, 1-CH_3), 2.52 (s, S-CH_3).

[Pb(SMeaaiNEt)$_2$I$_2$] (5b): Anal. found: C, 30.21; H, 2.93; N, 11.76 %. Calc. for $PbC_{24}H_{28}N_8S_2I_2$: C, 30.22; H, 2.94; N, 11.75 %. **FT-IR** (KBr disc), ν(N=N), 1414; ν(C=N), 1532 cm^{-1}. **UV/Vis** (DMF) (λ_{max}(nm)(10^{-3} ε (dm^3 mol^{-1} cm^{-1}): 361(27.32), 410(17.23). **^{1}H NMR** (300 MHz, $CDCl_3$), δ(ppm), (J(Hz)): 7.40 (br. s, 4-H), 7.23 (br. s, 5-H), 7.34 (d, 7.0 Hz, 8-H), 7.56 (m, 9- and 10-H), 7.82 (d, 8.0 Hz,11-H), 4.51 (q, 7.0 Hz, 1-CH_2), 1.63 (t, 7.3 Hz, (1-CH_2)-CH_3)), 2.59 (s, S-CH_3).

[Pb(SEtaaiNMe)$_2$I$_2$] (5c): Anal. found: C, 30.23; H, 2.95; N, 11.76 %. Calc. for $PbC_{24}H_{28}N_8S_2Cl_2$: C, 30.22; H, 2.94; N, 11.75 %. **FT-IR** (KBr disc), ν(N=N), 1413; ν(C=N), 1534 cm^{-1}. **UV/Vis** (CH_3CN) (λ_{max}(nm)(10^{-3} ε (dm^3 mol^{-1} cm^{-1}): 360(25.21), 412(17.88). **^{1}H NMR** (300 MHz, $CDCl_3$), δ(ppm), (J(Hz)): 7.43 (br. s, 4-H), 7.27 (br. s, 5-H), 7.32 (d, 7.0 Hz, 8-H), 7.55 (m, 9- and 10-H), 7.81 (d, 8.0 Hz, 11-H), 4.17 (s, 1-CH_3), 3.00 (q, 7.3 Hz, S-CH_2), 1.29 (t, 7.0 Hz, (S-CH_2)-CH_3).

[Pb(SEtaaiNEt)$_2$I$_2$] (5d): Anal. found: C, 31.79; H, 3.27; N, 11.40 %. Calc. for $PbC_{26}H_{32}N_8S_2I_2$: C, 31.80; H, 3.26; N, 11.41 %. **FT-IR** (KBr disc), ν(N=N), 1415; ν(C=N), 1533 cm^{-1}. **UV/Vis** (CH_3CN) (λ_{max}(nm) (10^{-3} ε (dm^3 mol^{-1} cm^{-1}): 362(28.11), 409(21.05). **^{1}H NMR** (300 MHz, $CDCl_3$), δ(ppm), (J(Hz)): 7.42 (br. s, 4-H), 7.22 (br. s, 5-H), 7.33 (d, 7.0 Hz, 8-H), 7.56 (m, 9- and 10-H), 7.80 (d, 8.0 Hz, 11-H), 4.44 (q, 7.30 Hz, 1-CH_2), 1.61 (t, 7.3 Hz, (1-CH_2)-CH_3), 3.05 (q, 7.4 Hz, S-CH_2), 1.30 (t, 5.30 Hz, (S-CH_2)-CH_3).

X-ray Diffraction

Single crystals suitable for data collection were grown from slow evaporation of the complexes in methanol. The crystal data and details of the data collections are given in Table 5. A suitable single crystal of [Pb(SEtaaiNEt)$_2$Cl$_2$] (**3d**) (0.26 × 0.22 × 0.20 mm) was mounted on a Bruker SMART APEX CCD diffractometer (graphite monochromated Mo-K_α radiation, λ = 0.71073 Å) and data were collected by use of ω scans. Unit cell parameters were determined from least-squares refinement of setting angles (θ) within the range 1.62 ≤ θ ≤ 25.73°. Out of 6087collected data 4584 were used for structure solution. The hkl ranges are –14 ≤ h ≤ 14, –13 ≤ k ≤ 14, –16 ≤ l ≤ 15. Data were corrected for Lorentz polarization effects and for linear decay. Semi-empirical absorption corrections based on ψ-scans were applied. The structures were solved by direct method using SHELXS-97[35] and successive difference Fourier syntheses. All non-hydrogen atoms were refined anisotropically. The hydrogen atoms were fixed geometrically and refined using the riding model. All calculation were carried out using SHELXL-97,[36] PLATON-99,[37] and ORTEP-32[38] programs.

Table 5. Summarized crystallographic data for [Pb(SEtaaiNEt)$_2$Cl$_2$] (**3d**).

	[Pb(SEtaaiNEt)$_2$Cl$_2$] (**3d**)
Empirical formula	$C_{26}H_{32}Cl_2N_8S_2Pb$
Formula weight	798.81
Temperature /K	293(2)
Crystal system	Triclinic
Space group	$P\bar{1}$
Crystal size /mm	0.26 × 0.22 × 0.20
Unit cell dimensions	
a /Å	11.691(5)
b /Å	12.083(5)
c /Å	13.185(5)
α /°	78.368(5)
β /°	72.962(5)
γ /°	67.843(5)
V /Å^3	1640.5(12)
Z	2
λ /Å	0.71073
μ (Mo-K_α) /mm^{-1}	5.461
D_{calc} /mg·m^{-3}	1.617
hkl range	–14 ≤ h ≤ 14, –13 ≤ k ≤ 14, –16 ≤ l ≤ 15
θ range /°	1.62–25.73
Refine parameters	346
Total reflection	6087
Unique data [$I > 2\sigma$ (I)]	4584
R_1[a] [$I > 2\sigma$ (I)]	0.0500
wR_2[b]	0.1409
Goodness of fit	1.017

a) $R = \Sigma|F_o - F_c|/\Sigma F_o$. b $wR = [\Sigma w(F_o^2 - F_c^2)/\Sigma wF_o^4]^{1/2}$ are general but w are different, $w = 1/[\sigma^2(F^2) + (0.0869P)^2]$ where $P = (F_o^2 + 2F_c^2)/3$.

Photometric Measurements

Absorption spectra were taken with a PerkinElmer Lambda 25 UV/Vis Spectrophotometer in a 1 × 1 cm quartz optical cell maintained at 25 °C with a Peltier thermostat. The light source of a PerkinElmer LS 55 spectrofluorimeter was used as an excitation light, with a slit width of 10 nm. An optical filter was used to cut off overtones when necessary. The absorption spectra of the *cis* isomers were obtained by extrapolation of the absorption spectra of a *cis*-rich mixture for which the composition is known from ^{1}H NMR integration. Quantum yields (ϕ) were obtained by measuring initial *trans*-to-*cis* isomerization rates (ν) in a well-stirred solution within the above instrument using the equation, $v = (\phi I_0/V)(1–10^{-Abs})$ where I_0 is the photon flux at the front of the cell, V is the volume of the solution, and Abs is the initial absorbance at the irradiation wavelength. The value of I_0 was obtained by using azobenzene (ϕ = 0.11 for π–π* excitation [39]) under the same irradiation conditions

The thermal *cis*-to-*trans* isomerization rates were obtained by monitoring absorption changes intermittently for a *cis*-rich solution kept in the dark at constant temperatures (T) in the range from 298–313 K. The activation energy (E_a) and the frequency factor (A) were obtained from the Arrhenius plot,

$$\ln k = \ln A – E_a/RT$$

where k is the measured rate constant, R is the gas constant, and T is temperature. The values of activation free energy (ΔG^*) and activation entropy (ΔS^*) were obtained through the relationships,

$$\Delta G^* = E_a – RT\text{-}T\Delta S^* \text{ and } \Delta S^* = [\ln A - 1 - \ln(k_B T/h)/R]$$

where k_B and h are Boltzmann's and Plank's constants respectively.

DFT and TD-DFT Calculations

The density functional theory (DFT) calculations on the crystal structures of $[Pb(SEtaaiNEt)_2Cl_2]$ (**3d**) has been carried out using the Gaussian 03w program package[40] with the aid of the GaussView visualization program.[41] The hybrid functional by Becke, B3LYP,[42] was used, which include a mixture of Hartree–Fock exchange with DFT exchange-correlation. We used 6-31G(d) basis set for C, H, N, Cl; 6-31+G(d) basis set for S, Br; LanL2DZ basis set including Los Alamos Effective Core Potentials I and Pb.[43–45]

Crystallographic data for the structure of $[Pb(SEtaaiNEt)_2Cl_2]$ (**3d**) have been deposited with the Cambridge Crystallographic Data center, CCDC No. 912370. Copies of this information may be obtained free of charge from the Director, CCDC, 12 Union Road, Cambridge CB2 1EZ, UK (E-mail: deposit@ccdc.cam.ac.uk or www:htpp://www.ccdc.cam.ac.uk).

Conclusion

Pb^{II} complexes of 1-alkyl-2-{(*o*-thioalkyl)phenylazo}imidazole (SRaaiNR') are described, $[Pb(SRaaiNR')_2X_2]$ (X = Cl, Br, I). The structures of the complexes have been confirmed by single-crystal X-ray structure study in representative cases. Photochromism of the complexes are examined by UV light irradiation in DMF solution and the results are compared with free ligands data. The decrease in electronegativity of X increases the rate of E-to-Z photoisomerization The Z-to-E isomerization is thermally driven process. The activation energy (E_as) of Z-to-E isomerization has been calculated. The slow rate of isomerization in complexes may be due to higher rotor volume than that of free ligands. DFT and TD-DFT computation using optimized geometry has supported experimental structure data and have explained spectral and photochromic properties.

Acknowledgments

Financial support from Department of Science & Technology, New Delhi is thankfully acknowledged.

References

[1] *Human Lead Exposure* (Ed.: H. L. Needleman), Boca Raton: CRC Press, **1992**.
[2] S. E. Manhan, *Environmental Chemistry*, 4th ed., Lewis Publishers, Boston, **1990**.
[3] J. E. Furgusson, *The Heavy Elements: Chemistry, Environmental Impact and Health Effects*, Pergamon Press, Oxford, **1990**.
[4] H. Zollinger, *Color chemistry: syntheses, properties and application of organic dyes and pigments*, 2nd ed. Weinheim: VCH, **1991**.
[5] G. Pavlovic, L. Racane, H. Cicak, V. Tralic-Kulenovic, *Dyes Pigm.* **2009**, *83*, 354–362.
[6] S. Kawata, Y. Kawata, *Chem. Rev.* **2000**, *100*, 1777–1788.
[7] J. A. Delaire, K. Nakatani, *Chem. Rev.* **2000**, *100*, 1817–1845.
[8] W. Huang, *Dyes Pigm.* **2008**, *79*, 69–75.
[9] N. Ertan, *Dyes Pigm.* **2000**, *44*, 41–48.
[10] I. Sener, F. Karc, N. Ertan, E. Kılıc, *Dyes Pigm.* **2006**, *70*, 143–148.
[11] F. Karc, N. Ertan, *Dyes Pigm.* **2002**, *55*, 99 –108.
[12] T. K. Misra, D. Das, C. Sinha, *Polyhedron* **1997**, *16*, 4163–4170.
[13] D. Mallick, A. Nandi, S. Datta, K. K. Sarker, T. K. Mondal, C. Sinha, *Polyhedron* **2012**, *31*, 506–514.
[14] G. Saha, P. Datta, K. K. Sarkar, R. Saha, G. Mostafa, C. Sinha, *Polyhedron* **2011**, *30*, 614–623.
[15] P. Datta, D. Sardar, P. Mitra, C. Sinha, *Polyhedron* **2011**, *30*, 1516–1523.
[16] T. K. Mondal, P. Raghavaiah, A. K. Patra, C. Sinha, *Inorg. Chem. Commun.* **2010**, *13*, 273–277.
[17] D. Das, A. K. Das, C. Sinha, *Talanta* **1999**, *48*, 1013–1022.
[18] P. Chattopadhyay, C. Sinha, D. K. Pal, *Fresenius J. Anal. Chem.* **1997**, *357*, 368–372.
[19] K. K. Sarker A. D. Jana, G. Mostafa, J.-S. Wu, T.-H. Lu, C. Sinha, *Inorg. Chim Acta* **2006**, *359*, 4377–4385.
[20] D. Mallick, K. K. Sarker, P. Datta, T. K. Mondal, C. Sinha, *Inorg. Chim. Acta* **2012**, *387*, 352–360.
[21] J. Otsuki, K. Suwa, K. Narutaki, C. Sinha, I. Yoshikawa, K. Araki, *J. Phys. Chem. A* **2005**, *109*, 8064–8069.
[22] K. K. Sarker, B. G. Chand, J. Cheng, T.-H. Lu, C. Sinha, *Inorg. Chem.* **2007**, *46*, 670–680.
[23] K. K. Sarker, D. Sardar, K. Suwa, J. Otsuki, C. Sinha, *Inorg. Chem.* **2007**, *46*, 8291–8301.
[24] K. K. Sarker, S. Saha Halder, D. Banerjee, T. K. Mondal, A. R. Paital, P. K. Nanda, P. Raghavaiah, C. Sinha, *Inorg. Chim. Acta* **2010**, *363*, 2955–2964.
[25] S. Saha Halder, P. Raghavaiah, C. Sinha, *Polyhedron* **2012**, *46*, 25–32.
[26] C. V. Yelamaggad, I. Shashikala, U. S. Hiremath, D. S. S. Rao, S. K. Prasad, *Liq. Cryst.* **2007**, *34*, 153–167.
[27] S. Kawata, Y. Kawata, *Chem. Rev.* **2000**, *100*, 1777–1788.
[28] E. Katz, A. N. Shipway, I. Willner, in *Photoreactive Organic Films* (Eds.: Z. Sekkat, W. Knoll), Academic Press, San Diego, **2002**, pp. 220–268.
[29] Special Issue: "Photochromism: Memories and Switches" (Ed.: M. Irie), *Chem. Rev.* **2000**, *100*, 1683–1890.
[30] *Organic Photochromic and Thermochromic Compounds* (Eds.: J. C. Crano, R. J. Guglielmetti), Kluwer Academic/Plenum Publishers, New York, NY, **1999**.
[31] *Photochromism: Molecules and Systems* (Eds.: H. Dürr, H. Bounas-Laurent), Elsevier: Amsterdam, **2003**.
[32] D. Banerjee, U. S. Ray, Sk. Jasimuddin, J.-C. Liou, T.-H. Lu, C. Sinha, *Polyhedron* **2006**, *25*, 1299–1306.
[33] A. J. Blake, D. Fenske, W.-S. Li, V. Lippolis, M. Schröder, *J. Chem. Soc., Dalton Trans.* **1998**, 3961–3968.
[34] J. Emsley, *The Elements*, 3rd edition, Oxford University Press, **1998**.
[35] G. M. Sheldrick, *SHELXS-97*, University of Gottingen, Germany, **1997**.
[36] G. M. Sheldrick, *SHELXL 97*, University of Gottingen, Germany, **1997**.
[37] L. J. Farrugia, ORTEP-3 for Windows, *J. Appl. Crystallogr.* **1997**, *30*, 565.
[38] A. L. Spek, *PLATON*, A Multipurpose Crystallographic Tool, Utrecht University, The Netherlands, **2001**.

[39] G. Zimmerman, L. Chow, U. Paik, *J. Am. Chem. Soc.* **1958**, *80*, 3528–3531.
[40] *Gaussian 03, Revision C.02*, M. J. Frisch, G. W. Trucks, H. B. Schlegel, G. E. Scuseria, M. A. Robb, J. R. Cheeseman, J. A. Montgomery Jr., T. Vreven, K. N. Kudin, J. C. Burant, J. M. Millam, S. S. Iyengar, J. Tomasi, V. Barone, B. Mennucci, M. Cossi, G. Scalmani, N. Rega, G. A. Petersson, H. Nakatsuji, M. Hada, M. Ehara, K. Toyota, R. Fukuda, J. Hasegawa, M. Ishida, T. Nakajima, Y. Honda, O. Kitao, H. Nakai, M. Klene, X. Li, J. E. Knox, H. P. Hratchian, J. B. Cross, V. Bakken, C.Adamo, J. Jaramillo, R. Gomperts, R. E. Stratmann, O. Yazyev, A. J. Austin, R. Cammi, C. Pomelli, J. W. Ochterski, P. Y. Ayala, K. Morokuma, G. A. Voth, P. Salvador, J. J. Dannenberg, V. G. Zakrzewski, S. Dapprich, A. D. Daniels, M. C. Strain, O. Farkas, D. K. Malick, A. D. Rabuck, K. Raghavachari, J. B. Foresman, J. V. Ortiz, Q. Cui, A. G. Baboul, S. Clifford, J. Cioslowski, B. B. Stefanov, G. Liu, A. Liashenko, P. Piskorz, I. Komaromi, R. L. Martin, D. J. Fox, T. Keith, M. A. Al-Laham, C. Y. Peng, A. Nanayakkara, M. Challacombe, P. M. W. Gill, B. Johnson, W. Chen, M. W. Wong, C. Gonzalez, J. A. Pople, Gaussian, Inc., Wallingford CT, **2004**.
[41] *GaussView, Version 3.09*, R. Dennington II, T. Keith, J. Millam, K. Eppinnett, W. L. Hovell, R. Gilliland, Semichem, Inc., Shawnee Mission, KS, **2003**.
[42] A. D. Becke, *J. Chem. Phys.* **1993**, *98*, 5648–5652.
[43] P. J. Hay, W. R. Wadt, *J. Chem. Phys.* **1985**, *82*, 270–283.
[44] W. R. Wadt, P. J. Hay, *J. Chem. Phys.* **1985**, *82*, 284–298.
[45] P. J. Hay, W. R. Wadt, *J. Chem. Phys.* **1985**, *82*, 299–310.

Received: March 26, 2013
Published Online: June 19, 2013

